



The use of Rietveld Method as a powerful tool for elucidating the anatase-to-rutile phase transition in titanium dioxide

Cruz N.A.¹, Cavaleiro A.A.¹, Stropa J.M.², Favarin L.R.V.², Machulek A.²,
Oliveira L.C.S.², Amoresi R.A.C.³, Zaghete M.A.³

¹(CDTEQ-Navirai, Universidade Estadual de Mato Grosso do Sul, Brazil)

²(INQUI, Universidade Federal de Mato Grosso do Sul, Brazil)

³(CDMF, Universidade Estadual Paulista, Brazil)

Abstract: Titanium dioxide semiconductor material has been extensively investigated for several purposes and several dopants has been inserted aiming new photonic properties. Several properties of titanium dioxide powders depend on the crystalline structure of anatase phase and some modifiers can be provide better or another characteristics. Some aspects of structural rearrangements in anatase phase can be satisfactorily evaluated by X-ray diffraction and Rietveld refinement in order to elucidate defect elimination and the basis of the anatase-to-rutile phase transition. By monitoring the lattice parameters along the temperature of thermal treatment, it is possible to understand the consequences of the dopant insertion and aid to propose new modification in the future. In this work, it was investigated the structural effects caused in anatase structure and in anatase-to-rutile phase transition by the simultaneous modification with 2 mol% of silicon and 4 mol% of zirconium homovalent modifiers. It was observed an effective stabilization of the anatase phase up to temperature as high as 900 °C besides the continuous increase of tetragonality.

Keywords: XRD characterization, Phase transition, Rietveld refinement, Sol-Gel synthesis

I. INTRODUCTION

Titanium dioxide TiO₂ is a semiconductor material extensively investigated for several purposes, but the synthesis procedures can lead to different crystalline phases, named anatase and rutile. The bare titanium dioxide powder possesses an expected anatase-to-rutile phase transition close to 600 °C since there are no significant organic residue originated from precursor reagents, which can lead to local overheating during the calcination step, besides the accentuated particle sintering [1-3]. Besides that, the anatase phase nucleation is a water-driven process and the cross-linked oxy-hydroxytitanium is essential to get the tetragonal phase with space group I41AmdZ. Thus, the Sol-Gel method based on acid hydrolysis seems to be the most applicable route to synthesize crystallized TiO₂ anatase single phase by thermal treatment close to 250 °C [4-7].

X-ray diffraction study aided by the Rietveld refinement is able to elucidate the main structural changes in crystalline TiO₂ samples. In general, some significant changes start to occur only when the annealing temperature exceeds 550 °C and no more structural rearrangements can be seen above 800 °C. The most accepted mechanism for anatase-to-rutile phase transition considers the structural consequences of the prior dehydroxylation process occurred during of thermal treatment at 250 °C. The hydroxyl group removal leads to formation of cross-linked nuclei with high amounts of oxygen vacancies in anatase phase, but the necessary energy for the oxygen reincorporation requires the breaking of titanium-oxygen bonds. However, the energy barrier of the anatase-to-rutile phase transition is similar to titanium-oxygen bond energy and both destroy-rebuilding processes leads to occurrence of the anatase-to-rutile phase transition besides the anatase phase crystallization. Because that, the oxygen supply during these events plays important rule in order to favor the crystallization of anatase phase [8-11].

The insertion of several dopants has been investigated in order to enhance the TiO₂ photonic properties in nanoparticles and thin films, but the samples are thermally treated at low temperatures only aiming to avoid the rutile formation [12-17]. However, the structural understanding for rutile ordering preference during the destroy-rebuilt process above 600 °C remains still to be found. The first clue to elucidate it is observed for titanium dioxide samples modified with homovalent cations, like the silicon IV [18-20] and zirconium IV ones [21-23]. Taking in account the hexacoordinated ionic radii for the tetravalent titanium, silicon and zirconium cations, it is possible to observe the ionic size mismatch is able to avoid the crystal symmetry gain involved into



anatase-to-rutile phase formation and anatase phase can be stabilized at higher temperatures than 600 °C. Nevertheless, the anatase crystallization is also avoided, which leads to lower crystalline powder samples.

By considering the silicon cation is smaller than titanium one, while the zirconium cation is bigger than the same titanium cation, all of them as hexacoordinated tetravalent cations in oxide structures, the average cation size mismatch can be reduced by simultaneous insertion of silicon and zirconium as dopant in titanium dioxide sample. The first attempt to perform that approach was made by Reidy et al. [24], but the published results did not contribute to the correct understanding of the anatase phase stabilization in titanium dioxide samples. By ionic radii simple calculations based on literature data [25], it was possible to find a weighted average value between hexacoordinated silicon (40 pm) and zirconium (72 pm) tetravalent cations close to titanium one (61 pm) and the $\text{Si}^{+4} : \text{Zr}^{+4}$ molar ratio was very close to 1 : 2. As consequence, the simultaneous insertion of $\text{Si}^{+4} : 2 \text{Zr}^{+4}$ cations can insert an appropriate local disorder in order to avoid the rutile crystal lattice in both silicon and zircon doped sites, but not to lead to long range distortions due to the opposite local distortion effect of each individual dopant.

In this work, silicon-zirconium (1 : 2) doped TiO_2 powder sample was obtained through the Sol-Gel method and compared to non-doped TiO_2 one, obtained in the same conditions. The dried gels were characterized by thermal analysis and the thermally treated samples from 500 to 900 °C for 2 hours were characterized by X-ray diffraction techniques followed by Rietveld refinement in order to elucidate several aspects involving the anatase-to-rutile phase transition.

II. MATERIAL AND METHODS

The synthesis of zirconium-silicon doped- TiO_2 powder sample was prepared with 2 mol% of silicon IV and 4 mol% of zirconium IV, according to nominal formula $\text{Si}_{0.02}\text{Zr}_{0.04}\text{Ti}_{0.94}\text{O}_2$ and compared with non-doped TiO_2 samples obtained in the same conditions. Both sample syntheses were carried out by the sol-gel method using metallic alkoxides with analytical grade purity in the presence of acetic acid as complexing agent. The molar ratio of acetic acid to metal cations was adjusted to 4:1 and the ethylic alcohol was used as solvent in order to adjust the total molar concentration to 1.0 mol L⁻¹. After the homogenization of initial precursors, it was added 10 % (V/V) of water acidified with HNO_3 at pH 3.0 in both solutions, aiming the slow controlled formation of metallic oxy-hydroxide nuclei. Both batch samples were stirred for 1 hour and let to jellify during 24 hours at room temperature.

The xerogel samples obtained in day after were dried at 100 °C for 24 hours, milled in a porcelain mortar and analyzed by simultaneous TG/DSC thermal analysis in TA instruments equipment, operating with synthetic air flow of 60 mL min⁻¹ and heating rate of 10 °C min⁻¹. Both dried gels were thermally treated at several temperatures from 500 to 900 °C for 2 hours in a muffle type oven and characterized by X-ray diffraction at room temperature from 20 to 90 ° (2-theta) degrees at 1° (2-theta)/min by using Bruker diffractometer, model D2 Phaser equipped with a monochromatic nickel filtered $\text{Cu K}\alpha$ radiation and LynxEye PSD detector. The collected diffraction patterns were used for phase identification, according to the JCPDS powder diffraction data bank [26] followed by structural model identification, according to the ICSD structural data bank [27] in order to carry out the Rietveld refinement [28] by using DBWS program [29]. Scanning Electron Microscopy was taken in a JSM-6380LV JEOL equipment, after gold sputtering.

III. RESULTS AND DISCUSSION

The thermal analyses of dried gels at 100 °C are shown in Fig. 1. On the top side are plotted TG curves and on the bottom the DSC ones. Both samples present a continuous weight loss starting from room temperature, which is higher for Si-Zr doped xerogel sample (2.2 % of weight loss) and ends also in higher temperature (340 °C), unlike the non-doped sample, which presents weight loss of 0.4 % and ends at 240 °C. In DSC curves is observed no energetic event below 100 °C, which permits to infer that weight loss is associated to volatile compounds dragging from analysis flow gas. The different amounts of these remaining compounds between the samples can be due to the sample porosity, which hinders the elimination of residues through volatilization. But, above 100 °C, an exothermic broad peak (I) can be observed for both samples, which is associated to the formation of cross-link Ti-O-Ti bonds by hydroxyl condensation.



No more weight losses were observed along the temperature increasing for both samples, which means there is no carbonaceous solid residues, which is expected to occur as weight loss around 400 °C. Thus, the thermal treatment at any temperature above 350 °C is able to eliminate ethanol (b.p. 77 °C), ethylic acetate ester (b.p. 78 °C), water (b.p. 100 °C) or acetic acid (b.p. 120 °C) residual compounds before the formation of cross-link Ti-O-Ti bonds.

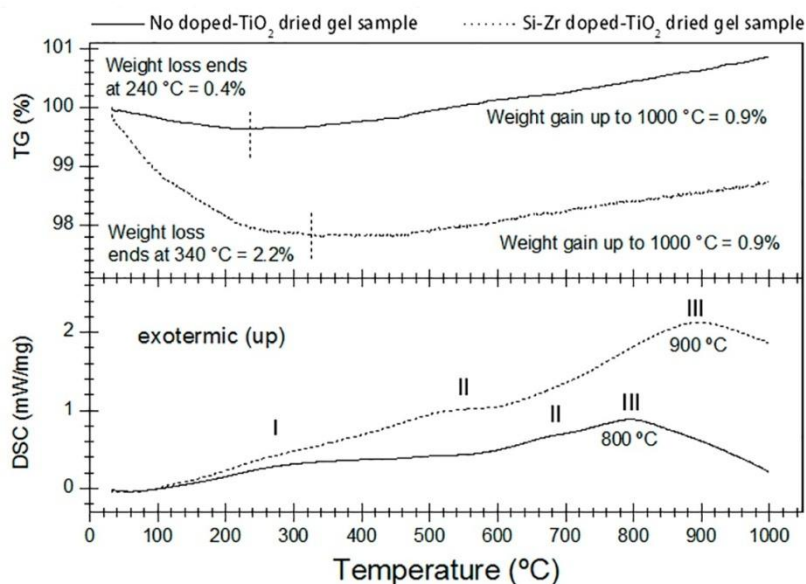


Figure 1: Thermal analysis (TG/DSC) of xerogel samples dried at 100 °C for 2 hours.

Taking in account the results of X-ray diffraction observed in Fig. 2, it is possible to interpret more accurately the weight gain region in thermal analysis. After the weight loss stage, is observed a weight gain for both samples, with differ in starting temperature, but not in weight gain amount. Both samples present 0.9 % in weight gain associated to oxygen incorporation until the final temperature of analysis at 1000 °C. The no doped xerogel sample present an exothermic broad peak at 800 °C (III), with a shoulder (II) starting from 600 °C. The peak II is associated to the initiation of the oxygen incorporation into anatase phase, which overlaps the subsequent anatase-to-rutile phase transition. By the other hand, the Si-Zr doped xerogel presents well defined process, with the initiation of the oxygen incorporation at 550 °C (II) and the anatase-to-rutile phase transition only at 900 °C (III).

The XRD patterns for no doped dried xerogel thermally treated at several temperatures are shown in Fig. 2.a. Below 700 °C there is no evidence of rutile phase and the diffraction peaks correspond to the (101), (004), (200), (105), (211), (204) and (106) main crystal planes, according to the JCPDS file 71-11166 [26]. The anatase-to-rutile phase transition can be verified for no doped samples thermally treated above 700 °C through the emergence of peaks at 27.4, 36.1 and 54.3 °(2-theta) degrees, correspondent to (110), (101), and (214) crystal planes, according JCPDS file 73-1232 [26]. These rutile referred peaks increase in intensity as a function of temperature of thermal treatment, reaching rutile single phase at 900 °C. By the other hand, the Zr-Si doped samples remain with anatase single phase along the entire temperature range, presenting the same peaks set observed for no-doped sample at lower temperatures.

In order to carry out the Rietveld refinement, the structural models were collected from ICSD data bank, where the anatase phase is associated to space group I41AmdZ, according card number 82084, and rutile one, to space group P42/mnm, according card number 53997 [27]. The refinement was performed through the pseudo-Voigt function for all of the samples and the results are shown in Fig 3.

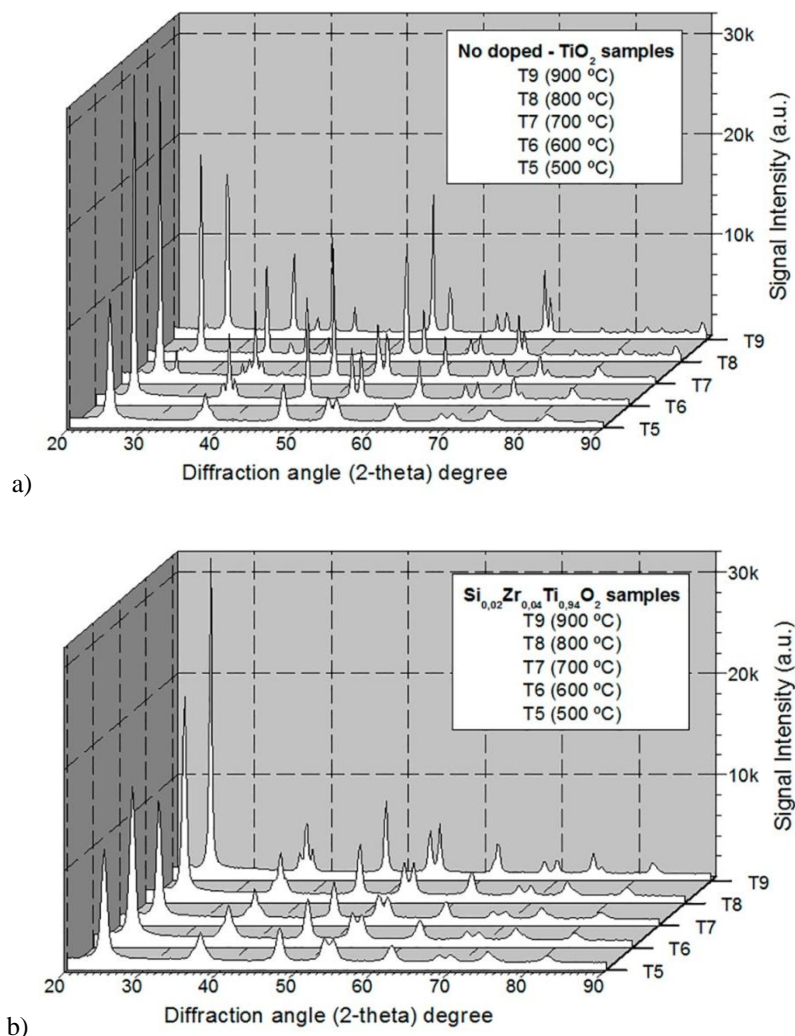


Figure 2: X-ray diffraction patterns for titanium dioxide powder samples thermally treated from 500 to 900 °C for 2 hours: a) nodoped-TiO₂ and b) Si_{0.02}Zr_{0.04}Ti_{0.94}O₂ samples.

The lattice parameters are presented in Fig.3.a, where is possible to observe the same variation profile for these parameters, which implicates the cell volume (Fig. 3.b) follow the same tendency along the temperature of thermal treatment. However, the tetragonality (*c/a* ratio) shown presented in Fig 3.b, shows a slight and continuous increasing for the Si-Zr doped-TiO₂ sample up to 900 °C, while a final decreasing occurs for nodoped sample after 700 °C, which is close to its complete vanishing from this temperature. The atomic coordinate for oxygen in I41AmdZ anatase structure tends to decreasing along the temperature of thermal treatment, firstly due the oxygen incorporation, after due the cell expansion together the rutile phase formation (Fig. 3.c). After the complete oxygen bond rebuilt above 800 °C the residual anatase phase suffer an strong cell contraction before due its complete vanishing, while the Si-Zr doped-TiO₂ sample remains with anatase single phase for entire process of thermal treatment.

The FWHM values for anatase phase are shown on the bottom of Fig. 3.c and are associated to simultaneous increase in crystallite size or decreasing in lattice microstrain. The FWHM values decrease pronouncedly for Si-Zr doped-TiO₂ sample, as consequence of anatase crystallization process. For no doped-TiO₂ sample, the FWHM value oscillates along the temperature of thermal treatment up to 800 °C, while the FWHM value for rutile phase starts with slightly lower value at 700 °C, remain practically invariable at 800 °C and decreases only at 900 °C, due the high crystallized rutile phase.



The silicon-zirconium dopant pair seems to be able to avoid the anatase phase transition due the delaying in the suppression of lattice microstrain, as expected as consequence of local ionic radii mismatch among titanium and the dopant pair and the crystallization process probably occurs as consequent of crystallite size increasing. That hypothesis is coherent with the no variation for FWHM values at high 2-theta angle, which is associated to lattice microstrain, while no is observed significant reduction for FWHM values at low 2-theta angle, associated to crystallite size.

SEM for some powder samples are shown in Fig. 4. Some agglomeration and significant porosity were evident in both powder samples at 500 °C and 900 °C. In addition, both samples thermally treated at 900 °C present more sintered particles in spite of no particle growth. Thus, the dopant pair seems does not change the typical powder morphology of the titanium dioxide.

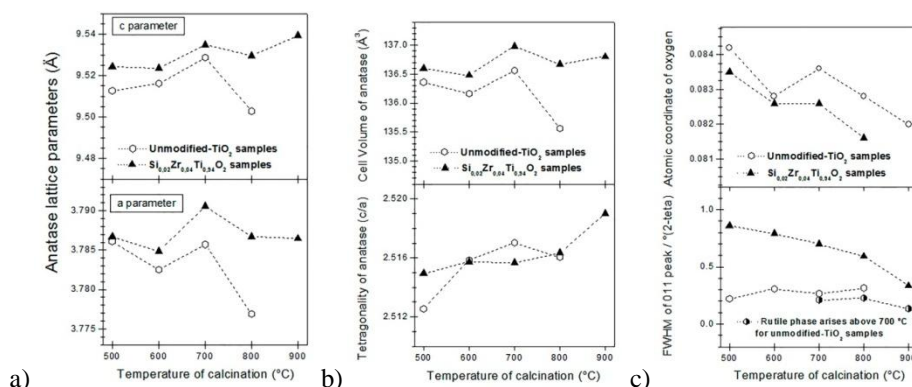


Figure 3: Refined data for refined anatase phase along the temperature of thermal treatment: a) lattice parameters, b) cell volume and tetragonality(c/a), c) atomic coordinate of oxygen atom and full width at half height (FWHM) plus correspondent values for rutile phase above 700 °C.

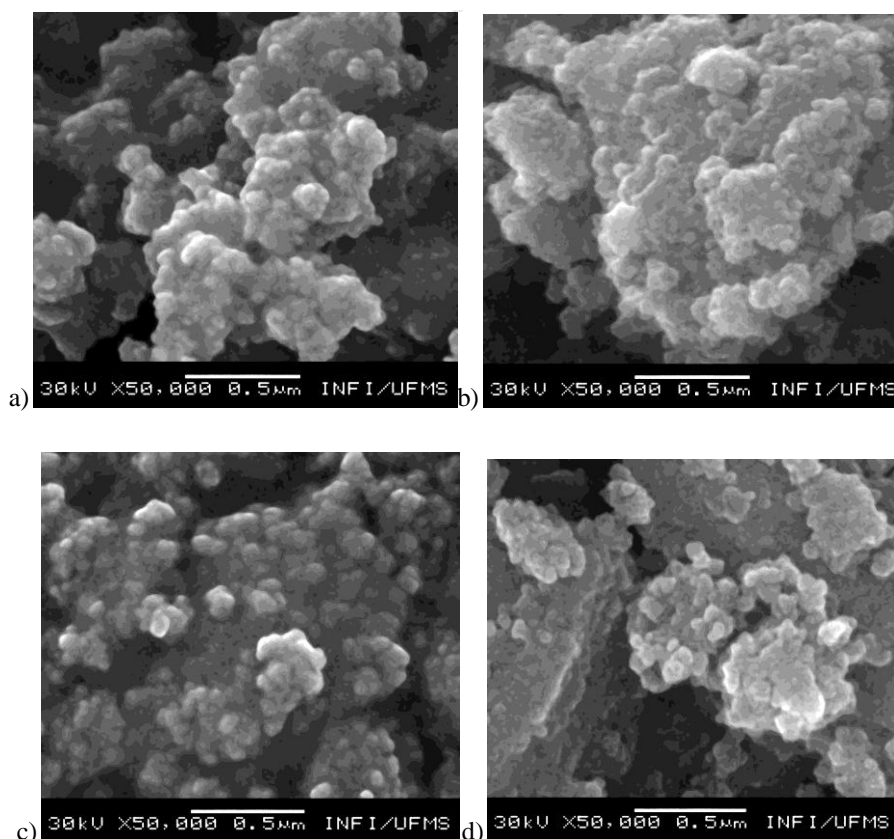


Figure 4: SEM images for TiO₂ powder samples thermally treated at: a) 500 and b) 900 °C, Si-Zr doped samples thermally treated at: c) 500 and d) 900 °C for 2 hours.



IV. CONCLUSION

In this study, we have successfully demonstrated the use of Rietveld method in order to elucidate some aspects of the anatase-to-rutile phase transition and as the silicon-zirconium dopant pair acts as anatase phase stabilizer. The oxygen incorporation associated to anatase defects elimination and consequent structural destroy-rebuilt process were verified for both compositions, but a consequent formation of rutile phase was only observed for no doped-TiO₂ one. The proposition the pair of homovalent modifiers like the silicon and zirconium tetravalent cations, was demonstrated can potential anatase phase stabilizer for Sol-Gel prepared powder samples, even after thermal treatment at higher temperature such 900 °C. The performed X-ray diffraction measurement and data suggests the occurrence of intrinsic changes even at low temperatures caused by doping process leads to continuous increasing in the tetragonality of anatase phase and its stabilization at high temperature of thermal treatment.

V. ACKNOWLEDGEMENTS

The authors thank the Brazilian foundations FUNDECT-MS, CNPq, CAPES and FINEP for financial supports.

REFERENCES

- [1] B. Li, X.Wang, M.Yan, and L.Li, Preparation and Characterization of Nano-TiO₂ Powder. *Materials Chemistry and Physics*, 78(1), 2002, 184-188.
- [2] S.A.Lopes, N.A.Cruz, D.C.Manfroi, R.G.Dias, M.S.Silva, M.A.Zaghet, A. Dos Anjos, A.A.Cavalheiro, and L.C.S.Oliveira, Effect of the Iron Doping on the Thermal Decomposition of the Polymeric Precursor for the Titanium Dioxide Powder Synthesis. *Materials Science Forum*, 798-799, 2014, 211-216.
- [3] D.A.H Hanaor, and C.C. Sorrell, Review of the Anatase to Rutile Phase Transformation. *Journal of Materials Science*, 46, 2011, 855-874.
- [4] A.A.Cavalheiro, J.C. Bruno, J.P.S. Valente, M.J. Saeki, and A.O.Florentino, Photocatalytic decomposition of diclofenac potassium using silver-modified TiO₂ thin films. *Thin Solid Films*, 516, 2008, 6240-6244.
- [5] O. Harizanov, and A. Harizanova. Development and Investigation of Sol-Gel Solutions for the Formation of TiO₂ Coatings. *Solar Energy Materials and Solar Cells*, 63(2), 2000, 185-195.
- [6] V.J. Nagpal, R.M. Davis, and J.S. Riffle, In Situ Steric Stabilization of Titanium Dioxide Particles Synthesized by a Sol-Gel Process. *Colloids and Surfaces A: Physicochemical and Engineering Aspects*, 87(1), 1994, 25-31.
- [7] A.A. Cavalheiro, L.C.S. Oliveira, and S.A.L. Santos, Structural Aspects of Anatase to Rutile Phase Transition in Titanium Dioxide Powders Elucidated by the Rietveld Method, in Dr. Magdalena Janus (Ed.), *Titanium Dioxide*, 3 (InTech, 2017) 63-81.
- [8] J.L. Look and D.F. Zukoski, Colloidal Stability and Titania Precipitate Morphology: Influence of Short-Range Repulsion. *Journal of the American Ceramic Society*, 78(1), 1995, 21-32.
- [9] M. Batzill, E.H. Morales, and U. Diebold, Influence of Nitrogen Doping on the Defect Formation and Surface Properties of TiO₂ Rutile and Anatase. *Physical Review Letters*, 96, 2006, 026103.
- [10] M. Salari, M. Rezaee, A.T. Chidembo, K. Konstantinov, and H. K. Liu, Rietveld Analysis of the Effect of Annealing Atmosphere on Phase Evolution of Nanocrystalline TiO₂ Powders. *Journal of Nanoscience and Nanotechnology*, 12 (6), 2012, 4724-4728.
- [11] Y. Hu, H.L. Tsai, and C.L. Huang, Phase Transformation of Precipitated TiO₂ Nanoparticles. *Materials Science and Engineering: A*, 344(1-2), 2003, 209-214.
- [12] S.Nadzirah, K.H. Foo, and U.Hashim, Morphological Reaction on the Different Stabilizers of Titanium Dioxide Nanoparticles. *International Journal of Electrochemical Science*, 10, 2015, 5498-5512.
- [13] A.A.Cavalheiro, J.C. Bruno, M.J. Saeki, O.S. Valente, and A.O.Florentino, Effect of Scandium on the Structural and Photocatalytic Properties of Titanium Dioxide Thin Films. *Journal of Materials Science*, 43(2), 2007, 602-608.
- [14] F. Mostaghni and Y. Abed, Structural Determination of Co/TiO₂ Nanocomposite: XRD Technique and Simulation Analysis. *Materials Science-Poland*, 3(3), 2016, 534-539.
- [15] W. Shu-Xin, M. Zhi, Q. Yong-Ning, H. Fei, J. Li-Shan, and Z. Yan-Jun, XPS Study of Cooper Doping TiO₂ Photocatalyst. *Acta Physico-Chimica Sinica*, 19(10), 2003, 967-969.



- [16] S. Liu, X. Liu, Y. Chen, and R. Jiang, A Novel Preparation of Highly Active Iron-Doped Titania Photocatalysts with a P-N Junction Semiconductor Structure, *Journal of Alloys and Compounds*, 506, 2010, 877-882.
- [17] N.N. Ilkhechi, and B.K. Kaleji, Effect of Cu^{2+} , Si^{4+} and Zr^{4+} Dopant on Structural, Optical and Photocatalytic Properties of Titania Nanopowders. *Optical and Quantum Electronics*, 48(347), 2016, 5-9.
- [18] F.A. Harraz, O.E. Abdel-Salam, A.A. Mostafa, R.M. Mohamed, and M. Hanafy, Rapid Synthesis of Titania-Silica Nanoparticles Photocatalyst by a Modified Sol-Gel Method for Cyanide Degradation and Heavy Metals Removal. *Journal of Alloys and Compounds*, 551, 2013, 1-7.
- [19] K. Okada, N. Yamamoto, Y. Kameshima, A. Yasumori, Effect of Silica Additive on the Anatase to Rutile Phase Transition. *Journal of the American Ceramic Society*, 84(7), 2001, 1591-1596.
- [20] Z. Ding, X. Hu, G.Q. Lu, P.-L. Yue, and P.F. Greenfield, Novel Silica Gel Supported TiO_2 Photocatalyst Synthesized by CVD Method. *Langmuir*, 16(15), 2000, 6216-6222.
- [21] S. Qiu, and T.L. Starr, Zirconium Doping in Titanium Oxide Photocatalytic Films Prepared by Atomic Layer Deposition. *Journal of the Electrochemical Society*, 154(6), 2007, H472-H475.
- [22] N.A. Badli, R. Ali, and L. Yuliati, Influence of Zirconium Doped Titanium Oxide towards Photocatalytic Activity of Paraquat. *Advanced Materials Research*, 1107, 2015, 377-382.
- [23] A. Kitiyanan, S. Ngamsinlapasathian, S. Pavasupree, and S. Yoshikawa, The Preparation and Characterization of Nanostructured TiO_2 - ZrO_2 Mixed Oxide Electrode for Efficient Dye-Sensitized Solar Cells. *Journal of Solid State Chemistry*, 178(4), 2005, 1044-1048.
- [24] D.J. Reidy, J.D. Holmes, and M.A. Morris, Preparation of a Highly Thermally Stable Titania Anatase Phase by Addition of Mixed Zirconia and Silica Dopants. *Ceramics International*, 32 (3), 2006, 235-239.
- [25] R.D. Shannon, Revised Effective Ionic Radii and Systematic Studies of Interatomic Distances in Halides and Chalcogenides. *Acta Crystallographica Section A, Foundations of Crystallographica*, A32, 1976, 751-767.
- [26] JCPDS - Joint Committee on Powder Diffraction Standards/International Center for Diffraction Data, Pennsylvania, Powder Diffraction File 2003.
- [27] ICSD - Inorganic Crystal Structure Database. Version 1.3.1, 2003.
- [28] H.M. Rietveld, A profile Refinement Method for Nuclear and Magnetic Structures. *Journal of Applied Crystallography*, 2, 1969, 65-71.
- [29] R.A. Young, A. Sakthivel, T.S. Moss, and C.O. Paiva-Santos, DBWS-9411 - an Upgrade of the DBWS Programs for Rietveld Refinement with PC and Mainframe Computers. *Journal of Applied Crystallography*, 28, 1995, 366-367.